arXiv:hep-ph/0701006v3 28 Mar 2007

# Transversity and Collins functions from SIDIS and $e^+e^-$ data

M. Anselmino,[1] M. Boglione,[1] U. D'Alesio,[2] A. Kotzinian,[3] F. Murgia,[2] A. Prokudin,[1] and C. Türk[1]

[1] *Dipartimento di Fisica Teorica, Università di Torino and INFN, Sezione di Torino, Via P. Giuria 1, I-10125 Torino, Italy*

[2] *Dipartimento di Fisica, Università di Cagliari and INFN, Sezione di Cagliari, C.P. 170, I-09042 Monserrato (CA), Italy*

[3] *Yerevan Physics Institute, 375036 Yerevan, Armenia, JINR, 141980 Dubna, Russia, and INFN, Sezione di Torino, Via P. Giuria 1, I-10125 Torino, Italy*

A global analysis of the experimental data on azimuthal asymmetries in semi-inclusive deep inelastic scattering (SIDIS), from the HERMES and COMPASS Collaborations, and in $e^+e^- \to h_1h_2X$ processes, from the Belle Collaboration, is performed. It results in the extraction of the Collins fragmentation function and, *for the first time*, of the transversity distribution function for $u$ and $d$ quarks. These turn out to have opposite signs and to be sizably smaller than their positivity bounds. Predictions for the azimuthal asymmetry $A_{UT}^{\sin(\phi_S+\phi_h)}$, as will soon be measured at JLab and COMPASS operating on a transversely polarized proton target, are then presented.

PACS numbers: 13.88.+e, 13.60.-r, 13.66.Bc, 13.85.Ni

## I. INTRODUCTION

The transversity distribution function, usually denoted as $h_{1q}(x,Q^2)$ or $\Delta_T q(x,Q^2)$, together with the unpolarized distribution functions $q(x,Q^2)$ and the helicity distributions $\Delta q(x,Q^2)$, contains basic and necessary information for a full understanding of the quark structure, in the collinear, $\boldsymbol{k}_\perp$ integrated configuration, of a polarized nucleon. The distribution of transversely polarized quarks in a transversely polarized nucleon, $\Delta_T q(x,Q^2)$, is so far unmeasured. The reason is that, being related to the expectation value of a chiral-odd quark operator, it appears in physical processes which require a quark helicity flip: this cannot be achieved in the usual inclusive DIS, due to the helicity conservation of perturbative QED and QCD processes.

The problem of measuring the transversity distribution has been largely discussed in the literature [1]. The most promising approach is considered the double transverse spin asymmetry $A_{TT}$ in Drell-Yan processes in $p\bar{p}$ interactions at a squared c.m. energy of the order of 200 GeV$^2$, which has been proposed by the PAX Collaboration [2, 3, 4, 5]. However, this requires the availability of polarized antiprotons, which is an interesting, but formidable task in itself. Meanwhile, the most accessible channel, which involves the convolution of the transversity distribution with the Collins fragmentation function [6], is the azimuthal asymmetry $A_{UT}^{\sin(\phi_S+\phi_h)}$ in SIDIS processes, namely $\ell\, p^\uparrow \to \ell\, \pi\, X$. This is the strategy being pursued by HERMES, COMPASS and JLab Collaborations.

A crucial improvement, towards the success of this strategy, has been recently achieved thanks to the independent measurement of the Collins function (or rather, of the convolution of two Collins functions), in $e^+e^- \to h_1h_2\,X$ unpolarized processes by Belle Collaboration at KEK [7]. By combining the SIDIS experimental data from HERMES [8, 9] and COMPASS [10], with the Belle data, we have, for the first time, a large enough set of data points as to attempt a global fit which involves, as unknown functions, both the transversity distributions and the Collins fragmentation functions of $u$ and $d$ quarks.

In Section II we briefly remind the basic formalism involved in the description of the SIDIS asymmetry $A_{UT}^{\sin(\phi_S+\phi_h)}$, and in Section III we develop, in somewhat greater detail, a similar formalism for the azimuthal correlations, involving two Collins functions, measured by Belle in $e^+e^- \to h_1h_2\,X$ processes. In Section IV we perform a global fit of HERMES [8, 9], COMPASS [10] and Belle [7] data, in order to extract *simultaneously* the Collins fragmentation function $\Delta^N D_{\pi/q^\uparrow}(z,p_\perp)$ and the transversity distribution function $\Delta_T q(x)$ for $q = u, d$. We then use, in Section V, the transversity distributions and the Collins functions so determined, to give predictions for forthcoming experiments at JLab and CERN-COMPASS. Comments and conclusions are gathered in Section VI.

## II. TRANSVERSITY AND COLLINS FUNCTIONS FROM SIDIS PROCESSES

The exact kinematics for SIDIS $\ell\, p \to \ell\, h\, X$ processes in the $\gamma^* - p$ c.m. frame, including all intrinsic motions, was extensively discussed in Ref. [11], and is schematically represented in Fig. 1. We take the virtual photon and the proton colliding along the $\hat{z}$-axis with momenta $\boldsymbol{q}$ and $\boldsymbol{P}$ respectively, and the leptonic plane to coincide with the $\hat{x}\hat{z}$ plane. We work in the kinematic regime in which $P_T \simeq \Lambda_{\rm QCD} \simeq k_\perp$, where $k_\perp$ is the magnitude of the intrinsic transverse momentum $\boldsymbol{k}_\perp$ of the initial quark with respect to the parent proton and $P_T = |\boldsymbol{P}_T|$ is the magnitude of the final hadron transverse momentum. We neglect second order corrections in the $k_\perp/Q$ expansion: in this approximation, the transverse momentum $\boldsymbol{p}_\perp$ of

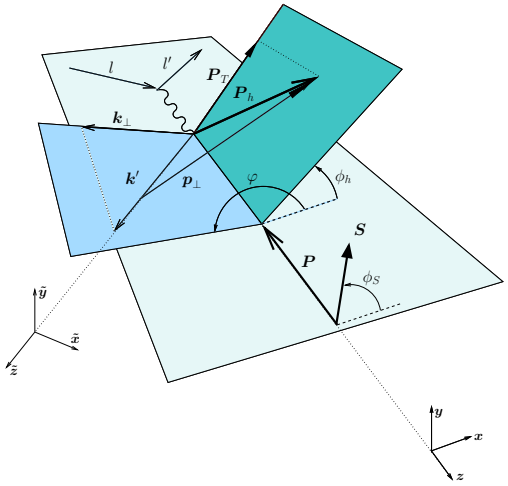


FIG. 1: Three dimensional kinematics of the SIDIS process, according to Trento conventions [14]. The photon and the proton collide along the $\hat{z}$-axis, while the leptonic plane defines the $\hat{x}\hat{z}$ plane. The fragmenting quark and the final hadron $h$ are emitted at azimuthal angles $\varphi$ and $\phi_h$, and the proton transverse spin direction is identified by $\phi_S$.

the observed hadron $h$ with respect to the direction of the fragmenting quark is related to $\boldsymbol{k}_\perp$ and $\boldsymbol{P}_T$ by the simple expression $\boldsymbol{p}_\perp = \boldsymbol{P}_T - z\boldsymbol{k}_\perp$; in addition, the light-cone momentum fractions $x$ and $z$ coincide with the usual measurable SIDIS variables, $z = z_h = (P\cdot P_h)/(P\cdot q)$ and $x = x_{_B} = Q^2/(2P\cdot q)$. In this region factorization holds [12, 13], leading order $\ell\, q \to \ell\, q$ elementary processes are dominating and the soft $P_T$ of the detected hadron is mainly originating from intrinsic motions.

The transverse single spin asymmetry (SSA) for this process is defined as

$$A_{_{UT}} = \frac{d^6\sigma^{\ell p^\uparrow\to\ell' h X} - d^6\sigma^{\ell p^\downarrow\to\ell' h X}}{d^6\sigma^{\ell p^\uparrow\to\ell' h X} + d^6\sigma^{\ell p^\downarrow\to\ell' h X}} \equiv \frac{d\sigma^\uparrow - d\sigma^\downarrow}{d\sigma^\uparrow + d\sigma^\downarrow}\,, \tag{1}$$

where $d^6\sigma^{\ell p^{\uparrow,\downarrow}\to\ell h X} \equiv d\sigma^{\uparrow,\downarrow}$ is a short hand notation for $(d^6\sigma^{\ell p^{\uparrow,\downarrow}\to\ell h X})/(dx_{_B}\, dy\, dz_h\, d^2\boldsymbol{P}_T\, d\phi_S)$. It will often happen, in comparing with data or giving measurable predictions, that the numerator and denominator of Eq. (1) will be integrated over some of the variables, according to the kinematical coverage of the experiments. $\uparrow$ and $\downarrow$ refer, respectively, to polarization vectors $\boldsymbol{S}$ and $-\boldsymbol{S}$, see Fig. 1. A full study of Eq. (1), with all contributions at all orders in $k_\perp/Q$, will be presented in a forthcoming paper [15].

We consider here, at $\mathcal{O}(k_\perp/Q)$, the $\sin(\phi_S+\phi_h)$ weighted asymmetry,

$$A_{_{UT}}^{\sin(\phi_S+\phi_h)} = 2\,\frac{\int d\phi_S\, d\phi_h\, [d\sigma^\uparrow - d\sigma^\downarrow]\,\sin(\phi_S+\phi_h)}{\int d\phi_S\, d\phi_h\, [d\sigma^\uparrow + d\sigma^\downarrow]}\,, \tag{2}$$

measured by the HERMES [8, 9] and COMPASS [10] Collaborations. This asymmetry singles out the spin dependent part of the fragmentation function of a transversely polarized quark with spin polarization $\hat{\boldsymbol{s}}$ and three-momentum $\boldsymbol{p}_q$:

$$\begin{aligned} D_{h/q,s}(z,\boldsymbol{p}_\perp) \;&=\; D_{h/q}(z,p_\perp) \\ &+\; \frac{1}{2}\,\Delta^N D_{h/q^\uparrow}(z,p_\perp)\,\hat{\boldsymbol{s}}\cdot(\hat{\boldsymbol{p}}_q\times\hat{\boldsymbol{p}}_\perp)\,, \end{aligned} \tag{3}$$

resulting in

$$A_{_{UT}}^{\sin(\phi_S+\phi_h)} = \frac{\displaystyle\sum_q e_q^2 \int d\phi_S\, d\phi_h\, d^2\boldsymbol{k}_\perp\, \Delta_T q(x,k_\perp)\,\frac{d(\Delta\hat\sigma)}{dy}\,\Delta^N D_{h/q^\uparrow}(z,p_\perp)\,\sin(\phi_S+\varphi+\phi_q^h)\,\sin(\phi_S+\phi_h)}{\displaystyle\sum_q e_q^2 \int d\phi_S\, d\phi_h\, d^2\boldsymbol{k}_\perp\, f_{q/p}(x,k_\perp)\,\frac{d\hat\sigma}{dy}\;D_{h/q}(z,p_\perp)}\,\cdot \tag{4}$$

In the above equation $\Delta_T q(x,k_\perp)$ is the unintegrated transversity distribution,

$$\Delta_T q(x) \equiv h_{1q}(x) = \int d^2\boldsymbol{k}_\perp\, \Delta_T q(x,k_\perp)\,, \tag{5}$$

while $\Delta^N D_{h/q^\uparrow}(z,p_\perp)$ is the Collins function, often denoted as [14]:

$$\Delta^N D_{h/q^\uparrow}(z,p_\perp) = \frac{2p_\perp}{zm_h}\, H_1^{\perp q}(z,p_\perp)\,. \tag{6}$$

$d\hat\sigma/dy$ is the planar unpolarized elementary cross section

$$\frac{d\hat\sigma}{dy} = \frac{2\pi\alpha^2}{sxy^2}\,[1+(1-y)^2]\,, \tag{7}$$

and

$$\frac{d(\Delta\hat\sigma)}{dy} = \frac{d\hat\sigma^{\ell q^\uparrow\to\ell q^\uparrow}}{dy} - \frac{d\hat\sigma^{\ell q^\uparrow\to\ell q^\downarrow}}{dy} = \frac{4\pi\alpha^2}{sxy^2}\,(1-y)\,\cdot \tag{8}$$

The $\sin(\phi_S+\varphi+\phi_q^h)$ azimuthal dependence in Eq. (4) arises from the combination of the phase factors in the transversity distribution function, in the non-planar

$\ell\, q \to \ell\, q$ elementary scattering amplitudes, and in the Collins fragmentation function; $\phi_S$ and $\varphi$ identify the directions of the proton spin $\boldsymbol{S}$ and of the quark intrinsic transverse momentum $\boldsymbol{k}_\perp$, see Fig. 1; $\phi_q^h$ is the azimuthal angle of the final hadron $h$, as defined in the fragmenting quark helicity frame. Neglecting $\mathcal{O}(k_\perp^2/Q^2)$ terms, one finds

$$\begin{aligned} \cos\phi_q^h &= \frac{P_T}{p_\perp}\,\cos(\phi_h-\varphi) - z\,\frac{k_\perp}{p_\perp}\,, \\ \sin\phi_q^h &= \frac{P_T}{p_\perp}\,\sin(\phi_h-\varphi)\,. \end{aligned} \tag{9}$$

A full study of Eq. (2), taking into account intrinsic motions with all contributions at all orders, following the general approach of Ref. [16], will be presented in a forthcoming paper [15]. Here, in agreement with all papers on the Collins effect in SIDIS so far appeared in the literature, we work at $\mathcal{O}(k_\perp/Q)$ and use Eqs. (4) and (9).

$f_{q/p}(x,k_\perp)$ is the unpolarized transverse momentum dependent (TMD) distribution function of a quark $q$ inside the parent proton $p$, while $D_{h/q}(z,p_\perp)$ is the unpolarized TMD fragmentation function of quark $q$ into the final hadron $h$. We assume the $k_\perp$ and $p_\perp$ dependences of these functions to be factorized in a Gaussian form, suitable to describe non-perturbative effects at small $P_T$ values and simple enough to allow analytical integration over the intrinsic transverse momenta:

$$f_{q/p}(x,k_\perp) = f_{q/p}(x)\,\frac{e^{-k_\perp^2/\langle k_\perp^2\rangle}}{\pi\langle k_\perp^2\rangle}\,, \tag{10}$$

$$D_{h/q}(z,p_\perp) = D_{h/q}(z)\,\frac{e^{-p_\perp^2/\langle p_\perp^2\rangle}}{\pi\langle p_\perp^2\rangle}\,, \tag{11}$$

where $f_{q/p}(x)$ and $D_{h/q}(z)$ are the usual integrated parton distribution and fragmentation functions, available in the literature; in particular we refer to Refs. [17, 18] and [19]. The QCD induced $Q^2$ dependence of these functions is also taken into account, although we do not indicate it explicitly. Finally, the average values of $k_\perp^2$ and $p_\perp^2$ are taken from Ref. [11], where they were obtained by fitting the azimuthal dependence of SIDIS unpolarized cross section:

$$\langle k_\perp^2\rangle = 0.25\ \mathrm{GeV}^2\,, \qquad \langle p_\perp^2\rangle = 0.20\ \mathrm{GeV}^2\,. \tag{12}$$

Notice that such values are assumed to be constant and flavor independent.

The transversity distributions and the Collins functions are unknown. We choose the following simple parameterization

$$\Delta_T q(x,k_\perp) = \frac{1}{2}\,\mathcal{N}_q^T(x)\,\left[f_{q/p}(x)+\Delta q(x)\right]\,\frac{e^{-k_\perp^2/\langle k_\perp^2\rangle_T}}{\pi\langle k_\perp^2\rangle_T}\,, \tag{13}$$

$$\Delta^N D_{h/q^\uparrow}(z,p_\perp) = 2\,\mathcal{N}_q^C(z)\,D_{h/q}(z)\,h(p_\perp)\,\frac{e^{-p_\perp^2/\langle p_\perp^2\rangle}}{\pi\langle p_\perp^2\rangle}\,, \tag{14}$$

with

$$\mathcal{N}_q^T(x) = N_q^T\,x^\alpha(1-x)^\beta\,\frac{(\alpha+\beta)^{(\alpha+\beta)}}{\alpha^\alpha\beta^\beta}\,, \tag{15}$$

$$\mathcal{N}_q^C(z) = N_q^C\,z^\gamma(1-z)^\delta\,\frac{(\gamma+\delta)^{(\gamma+\delta)}}{\gamma^\gamma\delta^\delta}\,, \tag{16}$$

$$h(p_\perp) = \sqrt{2e}\,\frac{p_\perp}{M}\,e^{-p_\perp^2/M^2}\,, \tag{17}$$

and $|N_q^T|,\ |N_q^C| \le 1$. In general $\langle k_\perp^2\rangle_T \neq \langle k_\perp^2\rangle$, but from our fits we learn that present experimental data are insensitive to such a difference, therefore we simply assume $\langle k_\perp^2\rangle_T = \langle k_\perp^2\rangle$. Also, in this first simultaneous extraction of the transversity and Collins functions, we let the coefficients $N_q^T$ and $N_q^C$ to be flavor dependent ($q=u,d$), while all the exponents $\alpha,\beta,\gamma,\delta$ and the dimensional parameter $M$ are taken to be flavor independent.

Notice that our parameterizations are devised in such a way that the transversity distribution function automatically obeys the Soffer bound [20]

$$|\Delta_T q(x)| \le \frac{1}{2}\,\left[f_{q/p}(x)+\Delta q(x)\right]\,, \tag{18}$$

and the Collins function satisfies the positivity bound

$$|\Delta^N D_{h/q^\uparrow}(z,p_\perp)| \le 2 D_{h/q}(z,p_\perp)\,, \tag{19}$$

since $\mathcal{N}_q^T(x)$, $\mathcal{N}_q^C(z)$ and $h(p_\perp)$ are normalized to be smaller than 1 in size for any value of $x$, $z$ and $p_\perp$ respectively.

By insertion of the above expressions into Eq. (4), we obtain, in agreement with Refs. [21, 22],

$$A_{UT}^{\sin(\phi_S+\phi_h)} = \frac{\dfrac{P_T}{M}\,\dfrac{1-y}{sxy^2}\,\sqrt{2e}\,\dfrac{\langle p_\perp^2\rangle_C^2}{\langle p_\perp^2\rangle}\,\dfrac{e^{-P_T^2/\langle P_T^2\rangle_C}}{\langle P_T^2\rangle_C^2}\,\displaystyle\sum_q e_q^2\,\mathcal{N}_q^T(x)\,\left[f_{q/p}(x)+\Delta q(x)\right]\,\mathcal{N}_q^C(z)\,D_{h/q}(z)}{\dfrac{e^{-P_T^2/\langle P_T^2\rangle}}{\langle P_T^2\rangle}\,\dfrac{[1+(1-y)^2]}{sxy^2}\,\displaystyle\sum_q e_q^2\,f_{q/p}(x)\,D_{h/q}(z)}\,, \tag{20}$$

where

$$\langle p_\perp^2\rangle_{_C} = \frac{M^2\langle p_\perp^2\rangle}{M^2+\langle p_\perp^2\rangle}\,, \qquad \langle P_T^2\rangle = \langle p_\perp^2\rangle + z^2\langle k_\perp^2\rangle\,, \qquad \langle P_T^2\rangle_{_C} = \langle z^2\rangle\left(\langle p_\perp^2\rangle_{_C} + \langle k_\perp^2\rangle\right) \tag{21}$$

Eq. (20) expresses $A_{_{UT}}^{\sin(\phi_S+\phi_h)}$ in terms of the parameters $\alpha, \beta, \gamma, \delta, N_q^T, N_q^C$ and $M$. In Section IV we shall fix them by performing a best fit of the measurements of HERMES, COMPASS and Belle Collaborations. Actually, we shall consider, following the experimental data, $A_{_{UT}}^{\sin(\phi_S+\phi_h)}$ as a function of one variable at a time, by properly integrating the numerator and denominator of Eq. (20): the integration over $x$ and $z$ gives the $P_T$ distribution of $A_{_{UT}}^{\sin(\phi_S+\phi_h)}$, whereas the integrations over $P_T$ and $z$ or $P_T$ and $x$, yield the $x$ and $z$ distributions. Notice that, with our approximations, $x = x_{_B}$ and $z = z_h$.

## III. COLLINS FUNCTIONS FROM $e^+e^-$ PROCESSES

The kinematics corresponding to the $e^+e^- \to h_1 h_2\, X$ process is schematically represented in Fig. 2: the two detected hadrons $h_1$ and $h_2$ are the fragmentation products of a quark and an antiquark originating from $e^+e^-$ collisions. We choose the reference frame so that the $e^+e^- \to q\,\bar q$ scattering occurs in the $\hat{x}\hat{z}$ plane, with the back-to-back quark and antiquark moving along the $\hat{z}$-axis. This choice requires, experimentally, the reconstruction of the jet thrust axis, but it involves a very simple kinematics and a direct contribution of the Collins functions, as we shall see. A different choice, originally suggested in the literature [23], is discussed at the end of this Section. In the configuration of Fig. 2, the four-momenta of the $e^+, e^-$ $(k^+, k^-)$ and of the $q, \bar q$ $(q_1, q_2)$ are

$$q_1 = \frac{\sqrt{s}}{2}(1,0,0,1)\,, \qquad q_2 = \frac{\sqrt{s}}{2}(1,0,0,-1)\,, \tag{22}$$
$$k^- = \frac{\sqrt{s}}{2}(1,-\sin\theta,0,\cos\theta)\,, \quad k^+ = \frac{\sqrt{s}}{2}(1,\sin\theta,0,-\cos\theta)\,.$$

The final hadrons $h_1$ and $h_2$ carry lightcone momentum fractions $z_1$ and $z_2$ and have intrinsic transverse momenta $\boldsymbol{p}_{\perp 1}$ and $\boldsymbol{p}_{\perp 2}$ with respect to the direction of fragmenting quarks,

$$\begin{aligned} \boldsymbol{p}_{\perp 1} &= p_{\perp 1}(\cos\varphi_1, \sin\varphi_1, 0)\,, \\ \boldsymbol{p}_{\perp 2} &= p_{\perp 2}(\cos\varphi_2, \sin\varphi_2, 0)\,, \end{aligned} \tag{23}$$

so that their four-momenta can be expressed as

$$\begin{aligned} P_1 &= \left(z_1\,\frac{\sqrt{s}}{2} + \frac{p_{\perp 1}^2}{2z_1\sqrt{s}}\,,\; p_{\perp 1}\,\cos\varphi_1\,,\; p_{\perp 1}\,\sin\varphi_1\,,\right. \\ &\qquad \left. z_1\,\frac{\sqrt{s}}{2} - \frac{p_{\perp 1}^2}{2z_1\sqrt{s}}\right), \\ P_2 &= \left(z_2\,\frac{\sqrt{s}}{2} + \frac{p_{\perp 2}^2}{2z_2\sqrt{s}}\,,\; p_{\perp 2}\,\cos\varphi_2\,,\; p_{\perp 2}\,\sin\varphi_2\,,\right. \\ &\qquad \left. -z_2\,\frac{\sqrt{s}}{2} + \frac{p_{\perp 2}^2}{2z_2\sqrt{s}}\right). \end{aligned} \tag{24}$$

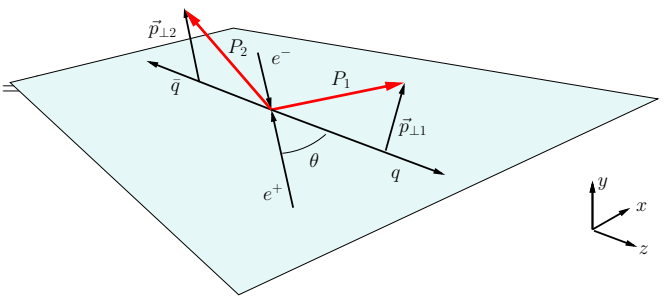


FIG. 2: Three dimensional kinematics of the $e^+e^- \to h_1 h_2\, X$ process, in the $q\,\bar q$ c.m. frame. In this configuration the reconstructed thrust axis identifies the $\hat{z}$-direction, the lepton-quark scattering plane defines the $\hat{x}\hat{z}$ plane.

At large c.m. energies and not too small values of $z$, one can neglect second order corrections in the $p_\perp/(z\sqrt{s})$ expansion, to work with the much simpler kinematics:

$$P_1 = \left(z_1\,\frac{\sqrt{s}}{2},\; p_{\perp 1}\cos\varphi_1,\; p_{\perp 1}\,\sin\varphi_1,\; z_1\,\frac{\sqrt{s}}{2}\right), \tag{26}$$

$$P_2 = \left(z_2\,\frac{\sqrt{s}}{2},\; p_{\perp 2}\,\cos\varphi_2,\; p_{\perp 2}\,\sin\varphi_2,\; -z_2\,\frac{\sqrt{s}}{2}\right). \tag{27}$$

Notice also that in this limit the lightcone momentum fractions $z$ coincide with the observable energy fractions $z_h$,

$$z_h = 2E_h/\sqrt{s} = z + \frac{p_\perp^2}{zs} \simeq z\,. \tag{28}$$

The cross section corresponding to this process, with unpolarized leptons, can be written as

$$\begin{aligned} \frac{d\sigma^{e^+e^-\to h_1h_2X}}{dz_1\,dz_2\,d^2\boldsymbol{p}_{\perp 1}\,d^2\boldsymbol{p}_{\perp 2}\,d\cos\theta} = \\ \frac{3}{32\pi s}\sum_q \frac{1}{4}\sum_{\{\lambda\}} \hat{M}_{\lambda_q\lambda_{\bar q};\lambda_+\lambda_-}\,\hat{M}^*_{\lambda'_q\lambda'_{\bar q};\lambda_+\lambda_-} \\ \times\, D^{h_1/q}_{\lambda_q\lambda'_q}(z_1,\boldsymbol{p}_{\perp 1})\, D^{h_2/\bar q}_{\lambda_{\bar q}\lambda'_{\bar q}}(z_2,\boldsymbol{p}_{\perp 2})\,, \end{aligned} \tag{29}$$

where $\hat{M}_{\lambda_q\lambda_{\bar q};\lambda_+\lambda_-}$ are the helicity amplitudes corresponding to the elementary scattering $e^+(\lambda_+)e^-(\lambda_-) \to q(\lambda_q)\bar q(\lambda_{\bar q})$, $q = u, \bar u, d, \bar d, s, \bar s$ (neglecting heavy flavors) and $\sum_{\{\lambda\}}$ indicates a sum over all helicity indices. In this case there are only two non-zero, independent amplitudes:

$$\begin{aligned} \hat{M}_{+-;+-} &= \hat{M}_{-+;-+} = e^2 e_q(1+\cos\theta)\,, \\ \hat{M}_{-+;+-} &= \hat{M}_{+-;-+} = e^2 e_q(1-\cos\theta)\,. \end{aligned} \tag{30}$$

The functions $D^{h_1/q}_{\lambda_q\lambda'_q}(z_1,\boldsymbol{p}_{\perp 1})$ and $D^{h_2/\bar q}_{\lambda_{\bar q}\lambda'_{\bar q}}(z_2,\boldsymbol{p}_{\perp 2})$ are the probability densities which describe the fragmentation

of quarks and antiquarks into the physical hadrons $h_1$ and $h_2$ respectively (see Section II.C of Ref. [16] for detailed explanations). In particular, the diagonal elements $D_{++}^{h/q}(z, \boldsymbol{p}_\perp)$ and $D_{--}^{h/q}(z, \boldsymbol{p}_\perp)$ correspond to the transverse momentum dependent unpolarized fragmentation function $D_{h/q}(z, p_\perp)$,

$$D_{++}^{h/q}(z, \boldsymbol{p}_\perp) = D_{--}^{h/q}(z, \boldsymbol{p}_\perp) = D_{h/q}(z, p_\perp)\,, \tag{31}$$

whereas the non-diagonal elements

$$\begin{aligned} D_{+-}^{h/q}(z, \boldsymbol{p}_\perp) &= D_{+-}^{h/q}(z, p_\perp)\, e^{i\varphi}\,, \\ D_{-+}^{h/q}(z, \boldsymbol{p}_\perp) &= D_{-+}^{h/q}(z, p_\perp)\, e^{-i\varphi} = -D_{+-}^{h/q}(z, p_\perp)\, e^{-i\varphi}\,, \end{aligned} \tag{32}$$

are related to the Collins fragmentation function $\Delta^N D_{h/q^\uparrow}(z, p_\perp)$ [11] by

$$\Delta^N D_{h/q^\uparrow}(z, p_\perp) = -2i\, D_{+-}^{h/q}(z, p_\perp) = 2i\, D_{-+}^{h/q}(z, p_\perp)\,. \tag{33}$$

The angle $\varphi$ in Eq. (33) is the azimuthal angle identifying the direction of the observed hadron $h$ in the helicity frame of the fragmenting quark $q$. Similar relations hold for the antiquark fragmentation functions, where one has to take into account a sign difference in $\varphi$ originating from the fact that the antiquark is chosen to move along the $-\hat{z}$ direction. Finally, inserting Eqs. (30)–(33) into Eq. (29) and performing the sum over the quark helicities one obtains

$$\begin{aligned} \frac{d\sigma^{e^+e^-\to h_1 h_2 X}}{dz_1\, dz_2\, d^2\boldsymbol{p}_{\perp 1}\, d^2\boldsymbol{p}_{\perp 2}\, d\cos\theta} &= \frac{3\pi\alpha^2}{2s} \sum_q e_q^2 \Big\{ (1+\cos^2\theta)\, D_{h_1/q}(z_1, p_{\perp 1})\, D_{h_2/\bar{q}}(z_2, p_{\perp 2}) \\ &+ \frac{1}{4}\, \sin^2\theta\, \Delta^N D_{h_1/q^\uparrow}(z_1, p_{\perp 1})\, \Delta^N D_{h_2/\bar{q}^\uparrow}(z_2, p_{\perp 2})\, \cos(\varphi_1+\varphi_2) \Big\}. \end{aligned} \tag{34}$$

Eq. (34) shows that the study of the correlated production of two hadrons (one for each jet) in unpolarized $e^+e^-$ collisions offers a direct access to the Collins functions, both regarding their $z$ and $p_\perp$ dependences. So far, only data on the $z$ dependence are available. Notice that by integrating over the intrinsic transverse momenta $\boldsymbol{p}_{\perp 1}$ and $\boldsymbol{p}_{\perp 2}$ one recovers the usual unpolarized cross section,

$$\begin{aligned} \frac{d\sigma^{e^+e^-\to h_1 h_2 X}}{dz_1\, dz_2\, d\cos\theta} &= \\ &\frac{3\pi\alpha^2}{2s}\,(1+\cos^2\theta) \sum_q e_q^2\, D_{h_1/q}(z_1)\, D_{h_2/\bar{q}}(z_2)\,, \end{aligned} \tag{35}$$

having used

$$\int d^2\boldsymbol{p}_\perp D_{h/q}(z, p_\perp) = D_{h/q}(z)\,. \tag{36}$$

To construct the physical observable measured by the Belle Collaboration, we now perform a change of angular variables from $(\varphi_1, \varphi_2)$ to $(\varphi_1, \varphi_1+\varphi_2)$ and then integrate over the moduli of the intrinsic transverse momenta, $p_{\perp 1}$ and $p_{\perp 2}$, and over the azimuthal angle $\varphi_1$. This leads to

$$\begin{aligned} \frac{d\sigma^{e^+e^-\to h_1 h_2 X}}{dz_1\, dz_2\, d\cos\theta\, d(\varphi_1+\varphi_2)} &= \frac{3\alpha^2}{4s} \sum_q e_q^2 \Big\{ (1+\cos^2\theta)\, D_{h_1/q}(z_1)\, D_{h_2/\bar{q}}(z_2) \\ &+ \frac{1}{4}\, \sin^2\theta\, \cos(\varphi_1+\varphi_2)\, \Delta^N D_{h_1/q^\uparrow}(z_1)\, \Delta^N D_{h_2/\bar{q}^\uparrow}(z_2) \Big\}\,, \end{aligned} \tag{37}$$

where we have defined

$$\int d^2\boldsymbol{p}_\perp \Delta^N D_{h/q^\uparrow}(z, p_\perp) \equiv \Delta^N D_{h/q^\uparrow}(z)\,. \tag{38}$$

By normalizing Eq. (37) to the azimuthal averaged cross section,

$$\langle d\sigma \rangle \equiv \frac{1}{2\pi}\, \frac{d\sigma^{e^+e^-\to h_1 h_2 X}}{dz_1\, dz_2\, d\cos\theta}$$

$$= \frac{3\alpha^2}{4s} \sum_q e_q^2 \,(1+\cos^2\theta)\, D_{h_1/q}(z_1)\, D_{h_2/\bar{q}}(z_2)\,, \quad (39)$$

one has

$$\begin{aligned} A(z_1,z_2,\theta,\varphi_1+\varphi_2) \;&\equiv\; \frac{1}{\langle d\sigma\rangle}\,\frac{d\sigma^{e^+e^-\to h_1h_2X}}{dz_1\,dz_2\,d\cos\theta\,d(\varphi_1+\varphi_2)} \\ &= 1+\frac{1}{4}\,\frac{\sin^2\theta}{1+\cos^2\theta}\,\cos(\varphi_1+\varphi_2) \\ &\times\frac{\sum_q e_q^2\,\Delta^N D_{h_1/q^\uparrow}(z_1)\,\Delta^N D_{h_2/\bar{q}^\uparrow}(z_2)}{\sum_q e_q^2 D_{h_1/q}(z_1)\,D_{h_2/\bar{q}}(z_2)}\,. \end{aligned} \quad (40)$$

Actually, Belle data are collected over a range of $\theta$ values, according to the acceptance of the detector (see Eq. (63)). Thus, Eqs. (37) and (39) are integrated over the covered $\theta$ range resulting in some specific $\langle\sin^2\theta\rangle$ and $\langle 1+\cos^2\theta\rangle$ values.

Finally, to eliminate false asymmetries, the Belle Collaboration considers the ratio of unlike-sign to like-sign pion pair production, $A_U$ and $A_L$, given by

$$\begin{aligned} R \;&\equiv\; \frac{A_U}{A_L} = \frac{1+\frac{1}{4}\,\cos(\varphi_1+\varphi_2)\,\frac{\langle\sin^2\theta\rangle}{\langle 1+\cos^2\theta\rangle}\,P_U}{1+\frac{1}{4}\,\cos(\varphi_1+\varphi_2)\,\frac{\langle\sin^2\theta\rangle}{\langle 1+\cos^2\theta\rangle}\,P_L} \\ &\simeq\; 1+\frac{1}{4}\,\cos(\varphi_1+\varphi_2)\frac{\langle\sin^2\theta\rangle}{\langle 1+\cos^2\theta\rangle}\,(P_U-P_L) \\ &\equiv\; 1+\cos(\varphi_1+\varphi_2)\,A_{12}(z_1,z_2)\,, \end{aligned} \quad (41)$$

with

$$P_U = \frac{\sum_q e_q^2\,[\Delta^N D_{\pi^+/q^\uparrow}(z_1)\,\Delta^N D_{\pi^-/\bar{q}^\uparrow}(z_2)+\Delta^N D_{\pi^-/q^\uparrow}(z_1)\,\Delta^N D_{\pi^+/\bar{q}^\uparrow}(z_2)]}{\sum_q e_q^2\,[D_{\pi^+/q}(z_1)\,D_{\pi^-/\bar{q}}(z_2)+D_{\pi^-/q}(z_1)\,D_{\pi^+/\bar{q}}(z_2)]}\,, \quad (42)$$

$$P_L = \frac{\sum_q e_q^2\,[\Delta^N D_{\pi^+/q^\uparrow}(z_1)\,\Delta^N D_{\pi^+/\bar{q}^\uparrow}(z_2)+\Delta^N D_{\pi^-/q^\uparrow}(z_1)\,\Delta^N D_{\pi^-/\bar{q}^\uparrow}(z_2)]}{\sum_q e_q^2\,[D_{\pi^+/q}(z_1)\,D_{\pi^+/\bar{q}}(z_2)+D_{\pi^-/q}(z_1)\,D_{\pi^-/\bar{q}}(z_2)]}\,, \quad (43)$$

$$A_{12}(z_1,z_2) = \frac{1}{4}\,\frac{\langle\sin^2\theta\rangle}{\langle 1+\cos^2\theta\rangle}\,(P_U-P_L)\,. \quad (44)$$

For fitting purposes, it is convenient to re-express $P_U$ and $P_L$ in terms of favoured and unfavoured fragmentation functions,

$$D_{\pi^+/u} = D_{\pi^+/\bar{d}} = D_{\pi^-/d} = D_{\pi^-/\bar{u}} \equiv D_{\rm fav}\,, \quad (45)$$

$$D_{\pi^+/d} = D_{\pi^+/\bar{u}} = D_{\pi^-/u} = D_{\pi^-/\bar{d}} = D_{\pi^\pm/s} = D_{\pi^\pm/\bar{s}} \equiv D_{\rm unf}, \quad (46)$$

and similarly for the $\Delta^N D$, obtaining

$$P_U = \frac{[5\,\Delta^N D_{\rm fav}(z_1)\,\Delta^N D_{\rm fav}(z_2)+7\,\Delta^N D_{\rm unf}(z_1)\,\Delta^N D_{\rm unf}(z_2)]}{[5\,D_{\rm fav}(z_1)\,D_{\rm fav}(z_2)+7\,D_{\rm unf}(z_1)\,D_{\rm unf}(z_2)]}\,, \quad (47)$$

$$P_L = \frac{[5\,\Delta^N D_{\rm fav}(z_1)\,\Delta^N D_{\rm unf}(z_2)+5\,\Delta^N D_{\rm unf}(z_1)\,\Delta^N D_{\rm fav}(z_2)+2\,\Delta^N D_{\rm unf}(z_1)\,\Delta^N D_{\rm unf}(z_2)]}{[5\,D_{\rm fav}(z_1)\,D_{\rm unf}(z_2)+5\,D_{\rm unf}(z_1)\,D_{\rm fav}(z_2)+2\,D_{\rm unf}(z_1)\,D_{\rm unf}(z_2)]}\,, \quad (48)$$

having neglected heavy quark contributions. $P_U$ and $P_L$ are the same as in Ref. [24], remembering Eq. (6) and noticing that

$$\begin{aligned} \Delta^N D_{h/q^\uparrow}(z) &= \int d^2\boldsymbol{p}_\perp \Delta^N D_{h/q^\uparrow}(z,p_\perp) \\ &= \int d^2\boldsymbol{p}_\perp \frac{2p_\perp}{zm_h}\,H_1^{\perp q}(z,p_\perp) = 4\,H_1^{\perp(1/2)q}(z)\,. \end{aligned} \quad (49)$$

In addition, the Belle Collaboration presents a second set of data, analysed in a different reference frame: following Ref. [23], one can fix the $\hat{z}$-axis as given by the direction of the observed hadron $h_2$ and the $\hat{xz}$ plane as determined by the lepton and the $h_2$ directions. There will then be another relevant plane, determined by $\hat{z}$ and the direction of the other observed hadron $h_1$, at an angle $\phi_1$ with respect to the $\hat{xz}$ plane. This kinematical configuration is shown in Fig. 3; it has the advantage that it does not require the reconstruction of the quark direction.

However, in this case the kinematics is more complicated. At first order in $p_\perp/(z\sqrt{s})$ one has

$$P_2 = |P_2|(1,0,0,-1)\,, \quad (50)$$

$$q_2 = \left(\frac{\sqrt{s}}{2}, -\frac{p_{\perp 2}}{z_2}\,\cos\varphi_2, -\frac{p_{\perp 2}}{z_2}\,\sin\varphi_2, -\frac{\sqrt{s}}{2}\right)\,, \quad (51)$$

$$q_1 = \left( \frac{\sqrt{s}}{2}, \frac{p_{\perp 2}}{z_2} \cos\varphi_2, \frac{p_{\perp 2}}{z_2} \sin\varphi_2, \frac{\sqrt{s}}{2} \right) , \tag{52}$$

$$\boldsymbol{P}_1 = \left( P_{1T} \cos\phi_1, P_{1T} \sin\phi_1, z_1 \frac{\sqrt{s}}{2} \right) , \tag{53}$$

$$\boldsymbol{p}_{\perp 1} = \left( P_{1T} \cos\phi_1 - \frac{z_1}{z_2} p_{\perp 2} \cos\varphi_2 , \right.$$
$$\left. P_{1T} \sin\phi_1 - \frac{z_1}{z_2} p_{\perp 2} \sin\varphi_2, \; 0 \right) . \tag{54}$$

Moreover, the elementary process $e^+e^- \to q\,\bar{q}$ does not occur in general in the $\hat{xz}$ plane, and thus the helicity scattering amplitudes involve an azimuthal phase $\varphi_2$. One can still perform an exact calculation, using the general approach discussed in Ref. [16]. A detailed description will be presented in a forthcoming paper [15]. We give here only the results valid at $\mathcal{O}(p_\perp/z\sqrt{s})$. The analogue of Eq. (34) now reads

$$\frac{d\sigma^{e^+e^-\to h_1 h_2 X}}{dz_1\, dz_2\, d^2\boldsymbol{p}_{\perp 1}\, d^2\boldsymbol{p}_{\perp 2}\, d\cos\theta_2} = \frac{3\pi\alpha^2}{2s} \sum_q e_q^2 \Big\{ (1+\cos^2\theta_2)\, D_{h_1/q}(z_1, p_{\perp 1})\, D_{h_2/\bar{q}}(z_2, p_{\perp 2}) \tag{55}$$
$$+ \frac{1}{4} \sin^2\theta_2\, \Delta^N D_{h_1/q^\uparrow}(z_1, p_{\perp 1})\, \Delta^N D_{h_2/\bar{q}^\uparrow}(z_2, p_{\perp 2}) \cos(2\varphi_2 + \phi_q^{h_1}) \Big\} ,$$

where $\phi_q^{h_1}$ is the azimuthal angle of the detected hadron $h_1$ around the direction of the parent fragmenting quark, $q$. Technically, $\phi_q^{h_1}$ is the azimuthal angle of $\boldsymbol{p}_{\perp 1}$ in the helicity frame of $q$. It can be expressed in terms of the integration variables we are using, $\boldsymbol{p}_{\perp 2}$ and $P_{1T}$. At lowest order in $p_\perp/(z\sqrt{s})$ we have

$$\cos\phi_q^{h_1} = \frac{P_{1T}}{p_{\perp 1}} \cos(\phi_1 - \varphi_2) - \frac{z_1}{z_2} \frac{p_{\perp 2}}{p_{\perp 1}} , \tag{56}$$

$$\sin\phi_q^{h_1} = \frac{P_{1T}}{p_{\perp 1}} \sin(\phi_1 - \varphi_2) . \tag{57}$$

Integrating Eq. (55) over $\boldsymbol{p}_{\perp 2}$ and $P_{1T}$, but not over $\phi_1$, and normalizing to the azimuthal averaged unpolarized cross section (39), we obtain the analogue of Eq. (40),

$$A(z_1, z_2, \theta_2, \phi_1) = 1 + \frac{1}{\pi} \frac{z_1\, z_2}{z_1^2 + z_2^2} \frac{\sin^2\theta_2}{1+\cos^2\theta_2} \cos(2\,\phi_1) \times \frac{\sum_q e_q^2\, \Delta^N D_{h_1/q^\uparrow}(z_1)\, \Delta^N D_{h_2/\bar{q}^\uparrow}(z_2)}{\sum_q e_q^2 D_{h_1/q}(z_1)\, D_{h_2/\bar{q}}(z_2)} , \tag{58}$$

in agreement with Ref. [24] taking into account the different notations, Eqs. (6) and (49).

Finally, Eq. (41) becomes in this configuration

$$R \simeq 1 + \cos(2\,\phi_1) A_0(z_1, z_2) , \tag{59}$$

with

$$A_0(z_1, z_2) = \frac{1}{\pi} \frac{z_1\, z_2}{z_1^2 + z_2^2} \frac{\langle \sin^2\theta_2 \rangle}{\langle 1+\cos^2\theta_2 \rangle} (P_U - P_L) , \tag{60}$$

where $P_U$ and $P_L$ are the same as defined in Eqs. (47) and (48).

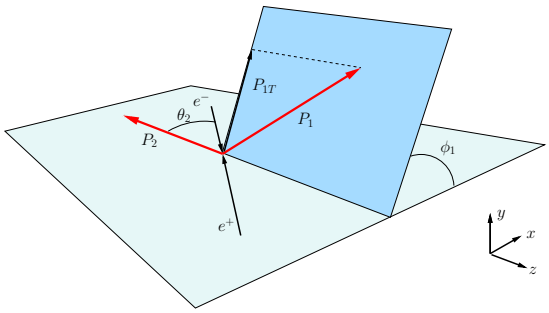


FIG. 3: Three dimensional kinematics of the $e^+e^- \to h_1 h_2\, X$ process. In this configuration the $\hat{z}$ direction is identified by the momentum of the final hadron $h_2$, while $h_1$ is emitted at an azimuthal angle $\phi_1$ with respect to the lepton-$h_2$ plane, defined as the $\hat{xz}$ plane.

## IV. TRANSVERSITY AND COLLINS FUNCTIONS FROM A GLOBAL FIT

We can now pursue our strategy of gathering simultaneous information on the transversity distribution function $\Delta_T q(x, k_\perp)$ and the Collins fragmentation function $\Delta^N D_{h/q^\uparrow}(z, p_\perp)$. To such a purpose we perform a global best fit analysis of experimental data involving these functions, namely the data from the SIDIS measurements by the HERMES [8, 9] and COMPASS [10] Collaborations, and the data from unpolarized $e^+e^- \to h_1 h_2\, X$ processes by the Belle Collaboration [7].

$\Delta_T q(x, k_\perp)$ and $\Delta^N D_{h/q^\uparrow}(z, p_\perp)$ are parameterized as shown in Eqs. (13)–(17). Considering the scarcity of data, in order to minimize the number of parameters, we assume flavor independent values of $\alpha$ and $\beta$ and, similarly, we assume that $\gamma$ and $\delta$ are the same for favored and unfavored Collins fragmentation functions, Eqs. (45) and (46); we then remain with a total number of 9 parameters. Their values, as determined through our global best

TABLE I: Best values of the free parameters for the $u$ and $d$ transversity distribution functions and for the favored and unfavored Collins fragmentation functions, Eqs. (13)-(17), as obtained by simultaneously fitting HERMES and COMPASS data on the $A_{UT}^{\sin(\phi_S+\phi_h)}$ asymmetry and the Belle data on the $A_{12}$ asymmetry, Eq. (44), proportional to $\cos(\varphi_1+\varphi_2)$. Notice that the errors generated by MINUIT are strongly correlated, and should not be taken at face value. The significant fluctuations in our results are shown by the shaded areas in Figs. 4, 5 and 6, as explained in the text. The values of $\langle k_\perp^2\rangle_T = \langle k_\perp^2\rangle$ and $\langle p_\perp^2\rangle$ are fixed, according to Eq. (12).

| FIT I ($A_{12}$) | | $\chi^2$/d.o.f. = 0.81 | | |
|---|---|---|---|---|
| Transversity | $N_u^T$ | $= 0.48 \pm 0.09$ | $N_d^T$ | $= -0.62 \pm 0.30$ |
| distribution | $\alpha$ | $= 1.14 \pm 0.68$ | $\beta$ | $= 4.74 \pm 5.45$ |
| function | $\langle k_\perp^2\rangle_T$ | $= 0.25$ GeV$^2$ | | |
| Collins | $N_{\rm fav}^C$ | $= 0.35 \pm 0.16$ | $N_{\rm unf}^C$ | $= -0.85 \pm 0.36$ |
| fragmentation | $\gamma$ | $= 1.14 \pm 0.38$ | $\delta$ | $= 0.14 \pm 0.36$ |
| function | $\langle p_\perp^2\rangle$ | $= 0.20$ GeV$^2$ | $M^2$ | $= 0.70 \pm 0.65$ GeV$^2$ |

TABLE II: Best values of the free parameters for the $u$ and $d$ transversity distribution functions and for the favored and unfavored Collins fragmentation functions, Eqs. (13)-(17), as obtained by simultaneously fitting HERMES and COMPASS data on the $A_{UT}^{\sin(\phi_S+\phi_h)}$ asymmetry and the Belle data on the $A_0$ asymmetry, Eq. (60), proportional to $\cos(2\phi_1)$. Notice that the errors generated by MINUIT are strongly correlated, and should not be taken at face value. The significant fluctuations in our results are shown by the shaded areas in Figs. 4, 5 and 6, as explained in the text. The values of $\langle k_\perp^2\rangle_T = \langle k_\perp^2\rangle$ and $\langle p_\perp^2\rangle$ are fixed, according to Eq. (12).

| FIT II ($A_0$) | | $\chi^2$/d.o.f. = 0.77 | | |
|---|---|---|---|---|
| Transversity | $N_u^T$ | $= 0.42 \pm 0.09$ | $N_d^T$ | $= -0.53 \pm 0.28$ |
| distribution | $\alpha$ | $= 1.20 \pm 0.83$ | $\beta$ | $= 5.09 \pm 5.87$ |
| function | $\langle k_\perp^2\rangle_T$ | $= 0.25$ GeV$^2$ | | |
| Collins | $N_{\rm fav}^C$ | $= 0.41 \pm 0.10$ | $N_{\rm unf}^C$ | $= -0.99 \pm 1.24$ |
| fragmentation | $\gamma$ | $= 0.81 \pm 0.40$ | $\delta$ | $= 0.02 \pm 0.37$ |
| function | $\langle p_\perp^2\rangle$ | $= 0.20$ GeV$^2$ | $M^2$ | $= 0.88 \pm 1.15$ GeV$^2$ |

fit are shown in Table I and II, together with the errors estimated by MINUIT.

As the two different sets of Belle data are based on a different analysis of the same experimental events, they are strongly correlated. Therefore, we have treated them separately in our combined analysis of the HERMES, COMPASS and Belle data; the best fit values of Table I are obtained by fitting the SIDIS results together with the Belle data on the $\cos(\varphi_1+\varphi_2)$ dependence, Eq. (41), while the values in Table II originate from the Belle data on the $\cos(2\phi_1)$ dependence, Eq. (59). We notice that the two sets of resulting best fit parameters are in full agreement within the uncertainties; this gives a good check of the consistency of the measurements and the stability of our analysis. In the sequel we shall present results and predictions based on the values of Table I; the corresponding results based on the values of Table II are hardly distinguishable (examples of this are shown explicitely in Fig. 6 and in Fig. 8, right panel).

Our best fits of the experimental data from HERMES, COMPASS and Belle are shown in Figs. 4, 5 and 6 respectively. The central curves correspond to the central values of the parameters in Table I, while the shaded areas correspond to one-sigma deviation at 90% CL and are calculated using the errors and the parameter correlation matrix generated by MINUIT, minimizing and maximizing the function under consideration, in a 9-dimensional parameter space hyper-volume corresponding to one-sigma deviation.

The transversity distribution functions $\Delta_T u(x,k_\perp)$ and $\Delta_T d(x,k_\perp)$ as resulting from our best fit – Eqs. (13)–(17) and Table I – are plotted as a function of $x$ and $k_\perp$ in Fig. 7; for comparison, the Soffer bound of Eq. (18) is also shown, as a bold line. The solid central line corresponds to the central values in Table I and the shaded area corresponds to the uncertainty in the parameter values, as explained above.

Similarly, the resulting Collins functions $\Delta^N D_{\rm fav}(z,p_\perp)$ and $\Delta^N D_{\rm unf}(z,p_\perp)$ are plotted as a function of $z$ – integrated over $d^2\boldsymbol{p}_\perp$, Eq. (49), and normalized to twice the unpolarized fragmentation functions – and as a function of $p_\perp$ in Fig. 8; for comparison, we also show the Collins functions from Refs. [24] and [25], respectively as dashed and dotted lines (left panels), and the corresponding positivity bound (19). The dashed lines in the right panels show the results corresponding to the parameters of Table II.

A few comments are in order.

- In Fig. 7 we show the extracted transversity distribution for $u$ and $d$ quarks. The $x$ dependence is based on the simple parameterization assumed in Eqs. (13) and (15), which contain $N_q^T, \alpha$ and $\beta$ as free parameters; our result represents the first extraction ever of the transversity distributions $\Delta_T u(x)$ and $\Delta_T d(x)$.

- The $k_\perp$ dependence has been assumed to be the same as for the unpolarized distributions. The flavor dependence is contained in the coefficients $N_q^T$ and in the proportionality of $\Delta_T q(x)$ to $[q(x) + \Delta q(x)]/2 = q_+^+(x)$, the number density of quarks with positive helicity inside a positive helicity proton.

- Our results show that the transversity distribution

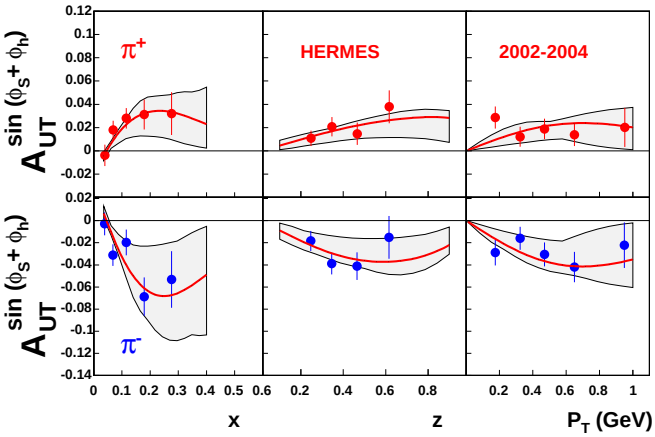


FIG. 4: HERMES experimental data [8, 9] on the azimuthal asymmetry $A_{UT}^{\sin(\phi_S+\phi_h)}$ for $\pi^{\pm}$ production are compared to the curves obtained from Eq. (20) with the parameterizations of Eqs. (13)-(17), and the parameter values, determined through our global best fit, given in Table I. The shaded area corresponds to the theoretical uncertainty on the parameters, as explained in the text.

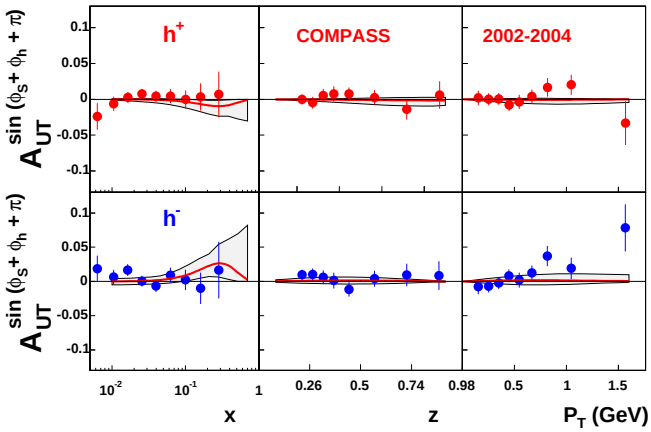


FIG. 5: The measurements of $A_{UT}^{\sin(\phi_S+\phi_h)}$, for the production of positively and negatively charged hadrons, from the COMPASS experiment operating on a deuterium target [10] are compared to the curves obtained from Eq. (20) with the parameterizations of Eqs. (13)-(17), and the parameter values, determined through our global best fit, given in Table I. The shaded area corresponds to the theoretical uncertainty on the parameters, as explained in the text. Notice the extra $\pi$ phase in addition to $\phi_S + \phi_h$ in the figure label, to keep into account the different choice of the Collins angle, with respect to Trento [14] and HERMES conventions, adopted by COMPASS Collaboration.

is positive for $u$ quarks and negative for $d$ quarks; the magnitude of $\Delta_T u$ is larger than that of $\Delta_T d$, while they are both significantly smaller than the corresponding Soffer bound.

- The shaded regions in Fig. 7 show that both $\Delta_T u(x, k_\perp)$ and $\Delta_T d(x, k_\perp)$ are, considering the limited amount of data, already well determined. It is worth noticing that while the HERMES data alone tightly constrain the transversity distribution of $u$ quarks, the addition of COMPASS data to the fit allows to better constrain the transversity distribution function of $d$ quarks. We have checked that fitting only HERMES and Belle data, ignoring the COMPASS results, still leads to a similar good $\chi^2$/d.o.f.; the resulting functions would give a slightly worse description – when compared to the global fit – of the $x$ dependence of $A_{UT}^{\sin(\phi_S+\phi_h)}$, as measured by COMPASS. This is mainly related to a less stringent determination of $\Delta_T d(x, k_\perp)$ in absence of deuteron target data. Although their measured azimuthal asymmetry is very small, the inclusion of COMPASS data significantly contributes to the extraction of the transversity distributions. Different fitting procedures were earlier attempted, for example by fixing $\Delta_T q = \Delta q$ or $\Delta_T q = q_+^+$ [26]: they lead to a slightly worse description of Belle data.

- The extracted Collins functions are shown in Fig. 8; they agree with similar extractions previously obtained in the literature [24, 25]. The shaded areas indicate well constrained Collins functions for $u$ and $d$ quarks in the large (valence) $z$ region, much smaller than their corresponding positivity bound.

- We note once more that, in analyzing SIDIS data, we have neglected the contributions of the sea quarks and antiquarks (assuming the corresponding transversity distributions in a proton to vanish), taking into account only $u$ and $d$ flavors. In analyzing Belle data and introducing the favored and unfavored Collins fragmentation functions, we have considered the contributions of $u, d$ and $s$ quarks, all abundantly produced in the $e^+e^-$ annihilation at $\sqrt{s} \simeq 10$ GeV.

- The partonic distribution and fragmentation functions are taken from Refs. [17, 18] and [19]. The QCD evolution is taken into account in the unpolarized distributions, in the unpolarized fragmentation functions and, following Ref. [27], for the transversity distributions.

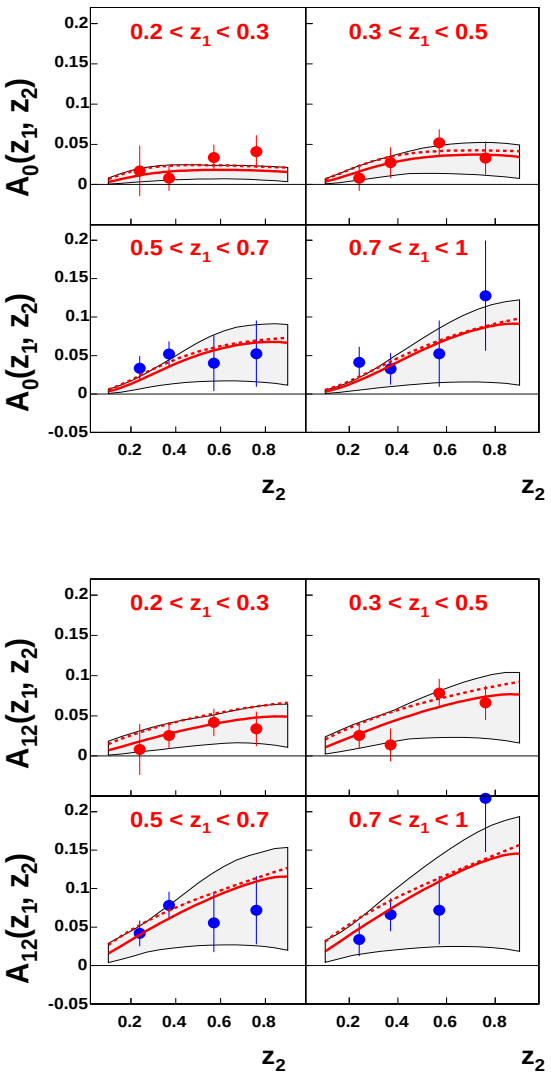


FIG. 6: The experimental data on two different azimuthal correlations in unpolarized $e^+e^- \to h_1 h_2 X$ processes, as measured by Belle Collaboration [7], are compared to the curves obtained from Eqs. (44) [$A_{12}$] and (60) [$A_0$] with the parameterizations of Eqs. (14), (16) and (17). The solid lines correspond to the parameters given in Table I, obtained by fitting the $A_{12}$ asymmetry; the shaded area corresponds to the theoretical uncertainty on these parameters, as explained in the text. The dashed lines correspond to the parameters given in Table II obtained by fitting the $A_0$ asymmetry. The agreement between the results obtained from the two fits shows the consistency between the two sets of Belle data and the solidity of our analysis.

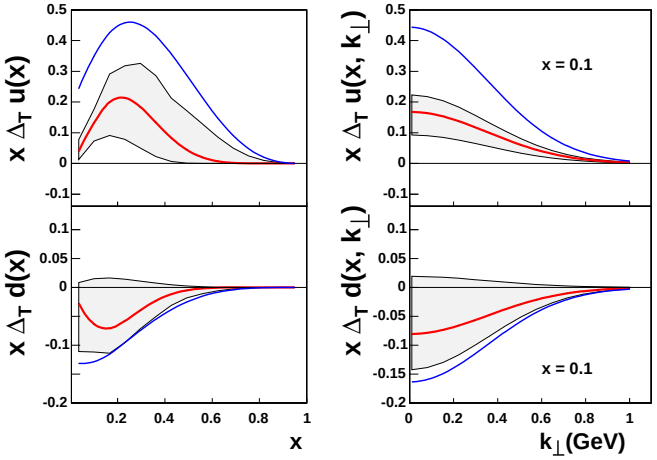


FIG. 7: The transversity distribution functions for $u$ and $d$ quarks as determined through our global best fit. In the left panel, $x\,\Delta_T u(x)$ (upper plot) and $x\,\Delta_T d(x)$ (lower plot), see Eq. (5), are shown as functions of $x$ and $Q^2 = 2.4$ GeV$^2$. The Soffer bound [20] is also shown for comparison (bold blue line). In the right panel we present the unintegrated transversity distributions, $x\,\Delta_T u(x, k_\perp)$ (upper plot) and $x\,\Delta_T d(x, k_\perp)$ (lower plot), as defined in Eq. (13), as functions of $k_\perp$ at a fixed value of $x$. Notice that this $k_\perp$ dependence is not obtained from the fit, but it has been chosen to be the same as that of the unpolarized distribution functions: we plot it in order to show its uncertainty (shaded area), due to the uncertainty in the determination of the free parameters.

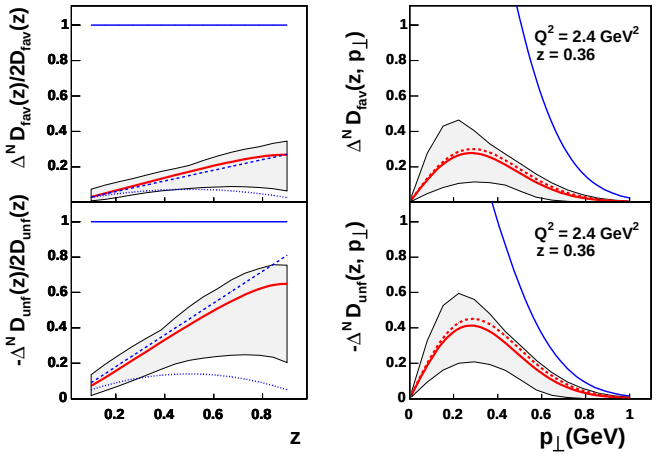


FIG. 8: Favored and unfavored Collins fragmentation functions as determined through our global best fit. In the left panel we show the $z$ dependence of the $p_\perp$ integrated Collins functions defined in Eq. (38) and normalized to twice the corresponding unpolarized fragmentation functions; we compare them to the results of Refs. [24] (dashed line) and [25] (dotted line). In the right panel we show the $p_\perp$ dependence of the Collins functions defined in Eq. (14), at a fixed value of $z$. The $Q^2$ value is 2.4 GeV$^2$, having assumed that the $Q^2$ evolution of $\Delta^N D$ is the same as that of $D$. The solid lines show the results based on the parameters of Table I, while the dashed ones show the results corresponding to the parameters of Table II. In all cases we also show the positivity bound (19) (upper lines).

Finally, we explicitly list, for clarity and completeness, the kinematical cuts we have imposed in numerical integrations, according to the setup of the HERMES experiment:

$$\begin{aligned} &0.2 \le z_h \le 0.7\,, \qquad &&0.023 \le x_B \le 0.4\,, \\ &0.1 \le y \le 0.85\,, \qquad &&Q^2 \ge 1\ \mathrm{GeV}^2\,, \\ &W^2 \ge 10\ \mathrm{GeV}^2\,, \qquad &&2 \le E_h \le 15\ \mathrm{GeV}\,, \end{aligned} \tag{61}$$

the COMPASS experiment:

$$\begin{aligned} &0.2 \le z_h \le 1\,, \qquad &&0.1 \le y \le 0.9\,, \\ &Q^2 \ge 1\ \mathrm{GeV}^2\,, \qquad &&W^2 \ge 25\ \mathrm{GeV}^2\,, \end{aligned} \tag{62}$$

and the Belle experiment

$$-0.6 \le \cos\theta_{\rm lab} \le 0.9\,, \qquad Q_T \le 3.5\ \mathrm{GeV}\,, \tag{63}$$

where $\theta_{\rm lab}$ is the polar production angle in the laboratory frame (related to the scattering angles $\theta$ and $\theta_2$ used in this paper) and $Q_T$ is the transverse momentum of the virtual photon from the $e^+e^-$ annihilation in the rest frame of the hadron pair [23].

## V. PREDICTIONS FOR ONGOING AND FUTURE EXPERIMENTS

We can now use the transversity distributions and the Collins functions we have obtained from fitting the available HERMES, COMPASS and Belle data, see Table I, to give predictions for new measurements planned by COMPASS and JLab Collaborations.

The transverse single spin asymmetry $A_{UT}^{\sin(\phi_S+\phi_h)}$ will be measured by the COMPASS experiment operating with a polarized hydrogen target (rather than a deuterium one). In Fig. 9 we show our predictions, obtained by adopting the same experimental cuts which were used for the deuterium target, see Eq. (62). Notice that this asymmetry is found to be sizeable, up to 5% in size.

The JLab experiments will measure $A_{UT}^{\sin(\phi_S+\phi_h)}$ for pion production off transversely polarized proton and neutron targets, at incident beam energies of either 6 or 12 GeV. The kinematical region spanned by these experiments is very interesting, as it will enable to explore the behavior of the transversity distribution function at large values of $x$, up to $x \sim 0.6$. The adopted experimental cuts for JLab operating on a proton target at 6 GeV are the following

$$\begin{aligned} &0.4 \le z_h \le 0.7, \qquad &&0.02 \le P_T \le 1\ \mathrm{GeV}, \\ &0.1 \le x_B \le 0.6, \qquad &&0.4 \le y \le 0.85, \\ &Q^2 \ge 1\ \mathrm{GeV}^2, \qquad &&W^2 \ge 4\ \mathrm{GeV}^2, \\ &1 \le E_h \le 4\ \mathrm{GeV}\,, \end{aligned} \tag{64}$$

whereas for a beam energy of 12 GeV they are

$$\begin{aligned} &0.4 \le z_h \le 0.7\ \ , \qquad &&0.02 \le P_T \le 1.4\ \mathrm{GeV}, \\ &0.05 \le x_B \le 0.7, \qquad &&0.2 \le y \le 0.85, \\ &Q^2 \ge 1\ \mathrm{GeV}^2, \qquad &&W^2 \ge 4\ \mathrm{GeV}^2, \\ &1 \le E_h \le 7\ \mathrm{GeV}\,. \end{aligned} \tag{65}$$

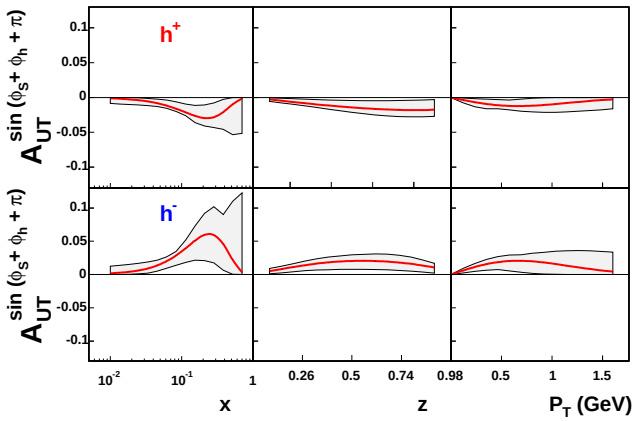


FIG. 9: Predictions for the single spin asymmetry $A_{UT}^{\sin(\phi_S+\phi_h)}$ as it will be measured by the COMPASS experiment operating with a transversely polarized hydrogen target. For the extra $\pi$ phase in the figure label see the caption of Fig. 5.

For a neutron target at 6 GeV the cuts read:

$$\begin{aligned} &0.46 \le z_h \le 0.59, \qquad &&0.13 \le x_B \le 0.40, \\ &0.68 \le y \le 0.86, \qquad &&1.3 \le Q^2 \le 3.1\ \mathrm{GeV}^2, \\ &5.4 \le W^2 \le 9.3\ \mathrm{GeV}^2, \qquad &&2.385 \le E_h \le 2.404\ \mathrm{GeV}\,, \end{aligned} \tag{66}$$

whereas for an incident beam energy of 12 GeV they are:

$$\begin{aligned} &0.3 \le z_h \le 0.7, \qquad &&0.05 \le x_B \le 0.55, \\ &0.34 \le y \le 0.9, \qquad &&Q^2 \ge 1\ \mathrm{GeV}^2, \\ &W^2 \ge 2.3\ \mathrm{GeV}^2\,. \end{aligned} \tag{67}$$

Our corresponding predictions, according to Eq. (20) and our extracted transversity and Collins functions, are shown in Figs. 10 and 11.

It is important to stress that, as the large $x$ region is not covered by the HERMES and COMPASS experiments, our predictions for the $x$ dependence of $A_{UT}^{\sin(\phi_S+\phi_h)}$ are very sensitive to the few available data points from HERMES and COMPASS at moderately large $x$ values. As a consequence, the predictions for the JLab experiments may vary drastically in the region $0.4 \le x_B \le 0.6$, as indicated by the large shaded area in Figs. 10 and 11. On the contrary, the results on the $P_T$ and $z_h$ dependences are more stable, as they only depend on the transversity distribution function integrated over $x$.

Finally, we compute the azimuthal asymmetry $A_{UT}^{\sin(\phi_S+\phi_h)}$ for the production of $K$ mesons and compare it with existing HERMES results [8, 9]. These data have not been included in our best fit, as they might involve the transversity distribution of strange quarks in the nucleon, which we have neglected for SIDIS data on $\pi$ production. We show our results in Fig. 12, obtained using the extracted $u$ and $d$ transversity distributions. Again, we have used favored ($\Delta^N D_{K^+/u^\uparrow}$) and unfavored ($\Delta^N D_{K^-/u^\uparrow}, \Delta^N D_{K^\pm/d^\uparrow}$) Collins functions, as in Eqs. (14), (16) and (17). For these we have used the same

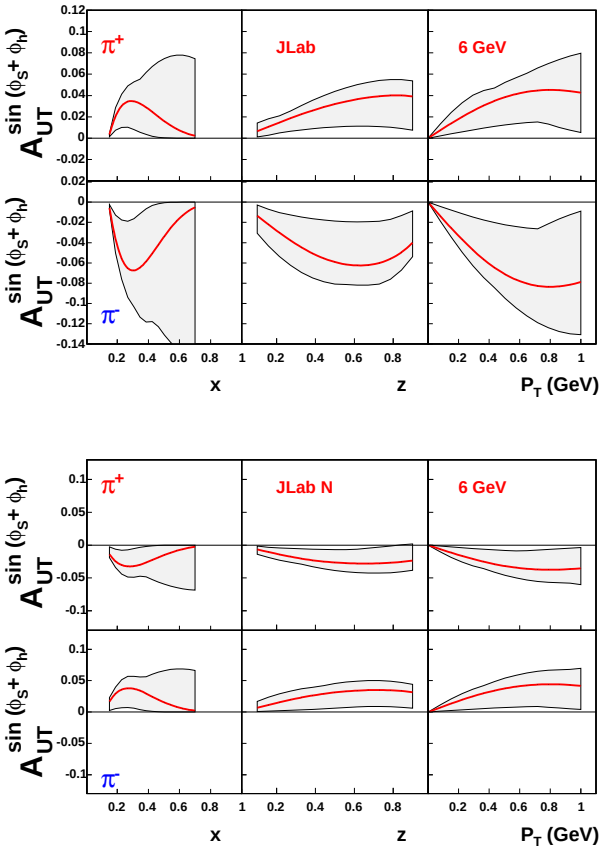





FIG. 10: Predictions for the single spin asymmetry $A_{UT}^{\sin(\phi_S+\phi_h)}$ as it will be measured at JLab operating on polarized hydrogen (proton, upper plot) and $He^3$ (neutron, lower plot) targets at a beam energy of 6 GeV.

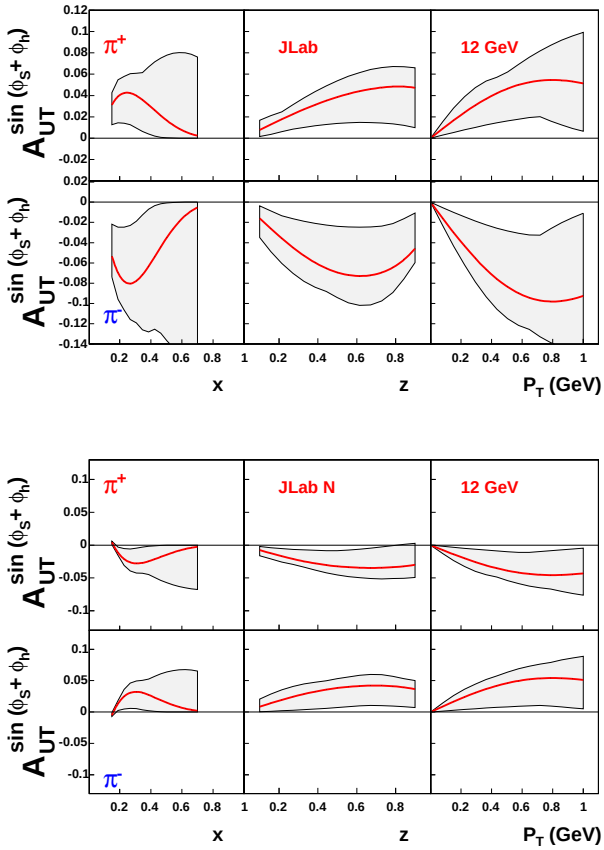





FIG. 11: Predictions for the single spin asymmetry $A_{UT}^{\sin(\phi_S+\phi_h)}$ as it will be measured at JLab operating on polarized hydrogen (proton, upper plot) and $He^3$ (neutron, lower plot) targets at a beam energy of 12 GeV.

parameters $N_q^C, \gamma, \delta$ and $M$ of Table I, with the appropriate unpolarized fragmentation functions $D_{K^\pm/q}$ [19].

We notice that our computations are in fair agreement with data concerning the $K^+$ production, which is presumably dominated by $u$ quarks; instead, there seem to be discrepancies for the $K^-$ asymmetry, for which the role of $s$ quarks might be relevant. New data on the azimuthal asymmetry for $K$ production, possible from COMPASS and JLab experiments, might be very helpful in sorting out the eventual importance of the sea quark transversity distributions in a nucleon.

## VI. COMMENTS AND CONCLUSIONS

We have performed a combined analysis of all experimental data on spin azimuthal asymmetries which involve the transversity distributions of $u$ and $d$ quarks and the Collins fragmentation functions, classified as favored (when the fragmenting quark is a valence quark for the final hadron) and unfavored (when the fragmenting quark is not a valence quark for the final hadron). We have fixed the total number of 9 parameters by best fitting the HERMES, COMPASS and Belle data.

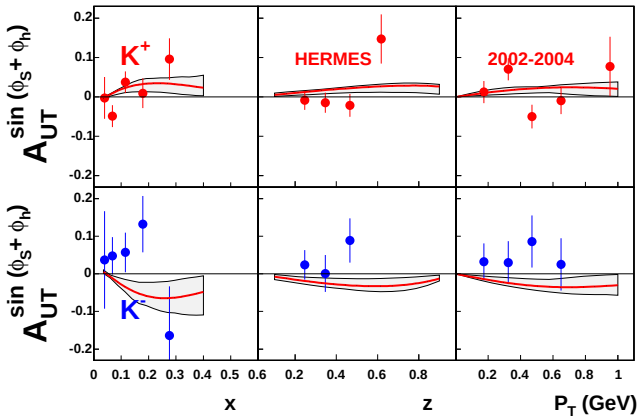


FIG. 12: Our results, based on the extracted transversity and Collins functions, for the azimuthal asymmetry $A_{UT}^{\sin(\phi_S+\phi_h)}$ for $K^\pm$ production, compared with the HERMES experimental data [8, 9].

All data can be accurately described, leading to the extraction of the favored and unfavored Collins functions, in agreement with similar results previously obtained in

the literature [24, 25]. In addition, we have obtained, *for the first time*, an extraction of the so far unknown transversity distributions for $u$ and $d$ quarks, $\Delta_T u(x)$ and $\Delta_T d(x)$. They turn out to be opposite in sign, with $|\Delta_T d(x)|$ smaller than $|\Delta_T u(x)|$, and both smaller than their Soffer bound [20].

The knowledge of the transversity distributions and the Collins fragmentation functions allows to compute the azimuthal asymmetry $A_{UT}^{\sin(\phi_S+\phi_h)}$ for any SIDIS process; we have then presented several predictions for incoming measurements from COMPASS and JLab experiments. They will provide further important tests of our complete understanding of the partonic properties which are at the origin of SSA. Data on $K$ production will help in disentangling the role of sea quarks.

Further expected data from Belle will allow to study in detail not only the $z$ dependence of the Collins functions, but also their $p_\perp$ dependence. The combination of data from SIDIS and $e^+e^- \to h_1 h_2 X$ processes opens the way to a new phenomenological approach to the study of the nucleon structure and of fundamental QCD properties, to be further pursued.

### Acknowledgments

We are grateful to Werner Vogelsang for supplying us with the numerical program for the QCD evolution of the transversity distributions.
We acknowledge the support of the European Community - Research Infrastructure Activity under the FP6 "Structuring the European Research Area" program (HadronPhysics, contract number RII3-CT-2004-506078).

[1] V. Barone, A. Drago, and P. G. Ratcliffe, Phys. Rept. **359**, 1 (2002).
[2] PAX Collaboration, V. Barone *et al.*, (2005), hep-ex/0505054.
[3] M. Anselmino, V. Barone, A. Drago, and N. N. Nikolaev, Phys. Lett. **B594**, 97 (2004).
[4] A. V. Efremov, K. Goeke, and P. Schweitzer, Eur. Phys. J. **C35**, 207 (2004).
[5] B. Pasquini, M. Pincetti, and S. Boffi, (2006), hep-ph/0612094.
[6] J. C. Collins, Nucl. Phys. **B396**, 161 (1993).
[7] Belle Collaboration, R. Seidl *et al.*, Phys. Rev. Lett. **96**, 232002 (2006).
[8] HERMES Collaboration, A. Airapetian *et al.*, Phys. Rev. Lett. **94**, 012002 (2005).
[9] HERMES Collaboration, L. Pappalardo *et al.*, in the proceedings of the XIV International Workshop on Deep Inelastic Scattering, Tsukuba city, Japan, April 20th - April 24th. (2006).
[10] COMPASS Collaboration, E. S. Ageev *et al.*, Nucl. Phys. **B765**, 31 (2007).
[11] M. Anselmino, M. Boglione, U. D'Alesio, A. Kotzinian, F. Murgia, A. Prokudin, Phys. Rev. **D71**, 074006 (2005).
[12] X.-d. Ji, J.-P. Ma, and F. Yuan, Phys. Lett. **B597**, 299 (2004).
[13] X.-d. Ji, J.-p. Ma, and F. Yuan, Phys. Rev. **D71**, 034005 (2005).
[14] A. Bacchetta, U. D'Alesio, M. Diehl, and C. A. Miller, Phys. Rev. **D70**, 117504 (2004).
[15] M. Anselmino, M. Boglione, U. D'Alesio, F. Murgia, and A. Prokudin, in preparation (2007).
[16] M. Anselmino, M. Boglione, U. D'Alesio, E. Leader, S. Melis, F. Murgia, Phys. Rev. **D73**, 014020 (2006).
[17] M. Gluck, E. Reya, and A. Vogt, Eur. Phys. J. **C5**, 461 (1998).
[18] M. Gluck, E. Reya, M. Stratmann, and W. Vogelsang, Phys. Rev. **D63**, 094005 (2001).
[19] S. Kretzer, Phys. Rev. **D62**, 054001 (2000).
[20] J. Soffer, Phys. Rev. Lett. **74**, 1292 (1995).
[21] A. Kotzinian, Nucl. Phys. **B441**, 234 (1995).
[22] P. J. Mulders and R. D. Tangerman, Nucl. Phys. **B461**, 197 (1996).
[23] D. Boer, R. Jakob, and P. J. Mulders, Nucl. Phys. **B504**, 345 (1997).
[24] A. V. Efremov, K. Goeke, and P. Schweitzer, Phys. Rev. **D73**, 094025 (2006).
[25] W. Vogelsang and F. Yuan, Phys. Rev. **D72**, 054028 (2005).
[26] A. Prokudin and C. Türk, (2006), hep-ph/0612087.
[27] O. Martin, A. Schäfer, M. Stratmann, and W. Vogelsang, Phys. Rev. **D57**, 3084 (1998).